
Proceedings Paper:
Saechan, P, Jaworski, AJ, Abbo, MS et al. (2017) Thermoacoustic refrigerator driven by a combustion-powered thermoacoustic engine for rural communities. In: Proceedings of ASEE17. International conference on advances in energy systems and environmental engineering (ASEE17), 02-05 Jul 2017, Wroclaw, Poland.

Thermoacoustic refrigerator driven by a combustion-powered thermoacoustic engine for rural communities

Patcharin Saechan[1], *Artur J.* Jaworski[2,*], *Mary S.* Abbo[3] , *Omar* Masera-Cerutti[4], and *Isares* Dhuchakallaya[5]

[1] Department of Mechanical and Aerospace Engineering, Faculty of Engineering, King Mongkut's University of Technology North Bangkok, 1518 Pracharat 1 Rd, Bangsue, Bangkok, 10800, Thailand
[2] Faculty of Engineering, University of Leeds, Leeds LS2 9JT, UK
[3] Centre for Research in Energy and Energy Conservation, located at College of Engineering, Design, Art and Technology, Makerere University, P.O. Box 7062, Kampala, Uganda
[4] Instituto de Investigaciones en Ecosistemas y Sustentabilidad, Antigua Carretera Patzcuaro No.8701, Col. Ex Hacienda San José de la Huerta, CP 58190, Morelia, Michoacan, Mexico
[5] Department of Mechanical Engineering, Faculty of Engineering, Thammasat University (Rangsit Campus), Khlong Luang, Pathumthani, 12121, Thailand

Abstract. The purpose of the current study is to present the potential of using coupled thermoacoustic engine/cooler in looped-tube topologies to be incorporated into designs of cookstoves in developing countries. This can be applied for storing vital medical supplies such as vaccines or agricultural produce in remote and rural communities. The usage of cookstoves in two sample rural communities of Mexico and Uganda is presented. Additionally, the low-cost coupled thermoacoustic engine/refrigerator system is demonstrated. The lowest temperature of -3.6°C, operating at frequency of 58.6 Hz, was achieved at the cold end of the refrigerator. Further numerical analysis of the thermoacoustic prototype is carried out to achieve a higher cooling performance. With the substantial adjustment, both regenerators of engine and refrigerator operate in the travelling wave phasing region with high acoustic impedance. The acoustic field in the system is also significantly improved. This will contribute to a better cooling performance of the system.

1 Introduction

Remote and rural communities in developing countries, especially in Africa and Asia, often face problems of no access to electrical energy. However, often they also require access to refrigeration capabilities for storing vital medical supplies such as vaccines or agricultural produce. In their daily life, the people in these societies cook on open fires with biomass burning, e.g. wood, charcoal, sawdust, etc [1]. This work aims at addressing the refrigeration needs by application of thermoacoustic technologies where thermal input from biomass

* Corresponding author: A.J.Jaworski@leeds.ac.uk

combustion can be used to directly generate acoustic power (in a thermoacoustic engine), which in turn can be converted to cooling power (in a coupled thermoacoustic refrigerator).

The energy conversion between thermal and acoustic energies relies on a thermoacoustic effect where the oscillation of a compressible working fluid in the vicinity of a solid material provides a means for designing thermodynamic cycles. Such technology is considered very attractive due to its reliability, low maintenance and environmental friendliness. Thermoacoustic devices can be classified into "engines" and "refrigerators/coolers/heat pumps". The thermoacoustic engine converts thermal energy into acoustic energy. Conversely, the thermoacoustic refrigerator employs an acoustic wave imposed along the solid material to generate the temperature gradient [2]. In recent years, there has been an increased research on the combined configuration of the thermoacoustic engine and refrigerator. The generated acoustic power from the engine can be supplied directly to produce the heat pumping effect in the refrigerator. The thermoacoustic refrigerator driven by the thermoacoustic engine also has particular advantages in using low-quality heat source or renewable energy, such as industrial waste heat, solar energy or flue gases from the combustion processes for energy recovery [3-6].

A demonstrator of a looped-tube travelling-wave thermoacoustic refrigerator driven by combustion-powered thermoacoustic engine has been developed [4]. It can be particularly beneficial for residents in remote and rural communities, where large quantities of waste heat are generated daily through biomass combustion in cookstoves. When such waste heat is harnessed to drive a cooling cycle it can be of immense benefit to improve the quality of healthcare by immediate access to vital medicines.

The purpose of the paper is two-fold: Firstly, to outline typical examples of cookstoves and their usage in two rural sample communities of Mexico and Uganda. Secondly, to explore the possibilities of using looped-tube topologies for coupled thermoacoustic engine/refrigerator to be incorporated into such cookstove designs. The prototype as discussed in [4] used standard inexpensive parts and employed air at atmospheric pressure as working fluid. The testing showed that the lowest temperature of -3.6°C was achieved at the cold end of the refrigerator. In the desired medicine storage temperature of +2 and +8°C, the system produced a cooling load between 3 and 7 W. Several aspects of the design are intensively examined for enhancing the cooling power by improving the phase difference between pressure and volumetric velocity, selecting suitable regenerators, and investigating the optimum position of the matching stub. This is demonstrated by modelling the system in DeltaEC programme. The cooling performance before and after the improvement is presented, and the changes to the acoustic field are examined.

2 The usage of cookstoves in rural communities

By way of illustration, it is worth mentioning two countries where use of cookstoves is relatively widespread: Mexico and Uganda. Biomass accounts for 10% of final energy use and 40% of residential energy use in Mexico. It is estimated that about 22.5 million people (or near 20% of Mexican total and 90% of rural population) still used fuelwood (FW) for cooking in open fires in 2010. Approximately 16.8 million people are exclusive users, and 5.7 million uses wood in combination with LPG (mixed use) to cover their cooking and other basic needs. Total fuelwood use reaches 310 PJ/yr or 40% of total residential sector energy use (763 PJ) [7].

Figures 1(a) and 1(b) illustrate two designs of cookstoves with chimney stacks where a significant amount of waste heat is discharged without making any use of it. Currently there are more than 100 stove manufacturers in Mexico, ranging from small-scale regional enterprises, to large-scale international manufacturers. Improved cookstoves in Mexico all come with a chimney and a flat pan to cook tortillas. They can be made of metal, or local

materials such as brick, cement and mud. There is therefore a lot of potential to incorporate cooler/refrigeration or electricity generation facilities (or both) as either a retrofit to existing designs or within the design of new stoves marketed in Mexico, for example within the government "top-down give-stoves-for-free approach" adopted by Mexican government within its Improved CookStove (ICS) programmes for rural communities.

The Ugandan energy sector is dominated by biomass, accounting for 92% of the energy use, followed by petroleum (6%) and electricity (2%) [8]. Biomass consumption comes from firewood, charcoal and crop residues. It provides all the basic needs for cooking and water heating in rural areas and for most urban households. The National Population and Housing Census 2014 [9] shows that biomass (wood and charcoal) are still used as main sources of energy for cooking by the vast majority of Ugandan households (94%). Use of electricity (2%) and gas (1%) is still very low, while about 3% of households use alternative fuel sources (biogas, cow dung, etc.) for cooking. Rural communities mainly use firewood (85%), followed by charcoal (12%), while urban communities show the opposite: charcoal (58%) as major energy source, followed by firewood (31%).

Ugandan manufacturers mainly rely on artisanal production methods which, though cheap, negatively affect product consistency and quality. There are a number of industrially produced cookstoves on the market, but they are all imported and at a higher price level. Highly advanced cooking solutions are available, though their penetration rate is currently quite low. However, the adoption by specific market segments of these modern cookstoves, that provide a combination of cooking, lighting and charging of mobile devices, may offer a good entry point for thermoacoustic devices in Uganda. Figure 1(c) illustrates an institutional stove at a prison facility in Uganda with a chimney stack where large quantities of waste heat are disposed to the atmosphere.

(a) (b) (c)

Fig. 1. Examples of cookstoves with chimney stacks: (a) and (b) rural dwellings in Mexico; (c) institutional stove at a prison's facility in Uganda

3 The coupled thermoacoustic engine/refrigerator

A prototype of looped-tube travelling wave thermoacoustic refrigerator driven by combustion-powered thermoacoustic engine [4] was developed. The system was designed with the requirements of a simple structure and low-cost device. The important design issues including type of the device, operating pressure, working fluid, material and configuration of each component are considered under those constrains.

To meet the simplicity and low-cost point of view, air at atmospheric pressure was selected as working fluid because of its availability. A one-wavelength looped-tube travelling

wave structure was designed because of providing relatively efficient energy conversion. Such a relatively simple arrangement could be implemented as a practical solution. In addition, an extra phase tuning component namely "a matching stub" was introduced into the system to improve the impedance matching of a "coupled" engine/refrigerator system. The matching stub is to shunt part of the velocity away from the resonator to compensate the acoustic impedance increase caused by the existence of the refrigerator inside the loop [10].

The schematic diagram of the system is presented in Fig. 2. There are two subsystems: the engine and the refrigerator, located in the same loop of a travelling wave type. The engine is powered by flue gases. It comprises of cold heat exchanger (CHX_e), regenerator (REG_e), hot heat exchanger (HHX_e), thermal buffer tube (TBT) and secondary cold heat exchanger ($2^{nd}CHX$). The refrigerator is located opposite to the engine and consists of an ambient heat exchanger (AHX_r), regenerator (REG_r) and cold heat exchanger (CHX_r). In addition, the side branch matching stub is used while the feedback pipes complete the loop. The total loop length is 4.969 m corresponding to an operating frequency of 58.6 Hz. Subscripts "e" and "r" refer to the engine and refrigerator, respectively. The coordinate x describing the distribution of components within the loop for modelling starts from the cold heat exchanger of the engine (CHX_e); x = 0.

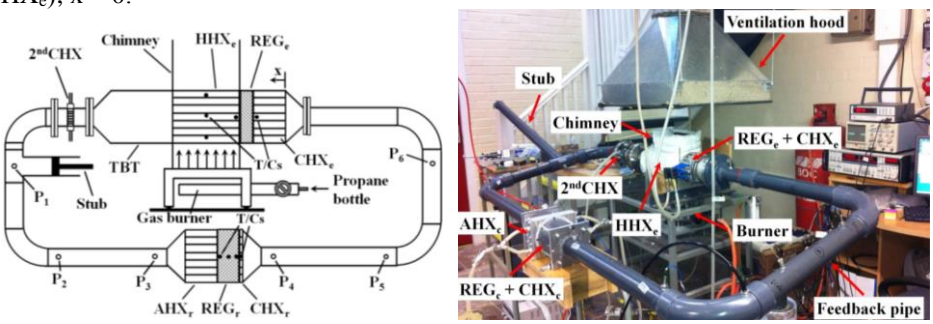

Fig. 2. Schematic diagram (left) and laboratory implementation (right) of the system [4]

In the thermoacoustic engine, the CHX_e is made from a round aluminium block which is 90 mm long and has 110 mm diameter. The porosity of the CHX_e is about 9.3%. The REG_e is made out of stainless screen disks with the diameter of 110 mm and the wire diameter of 0.16 mm. The length of the REG_e is 23 mm. The porosity and hydraulic radius of the REG_e are 82% and 196 μm, respectively. Two Type-K thermocouples are installed at the two ends of the REG_e to monitor the temperature difference. The HHX_e has a shell-and-tube configuration and has a length of 160 mm. It is heated by the combustion process. Three Type-K thermocouples are placed in the HHX_e to monitor the solid temperature of the tube wall. The TBTs are located between the HHX_e and $2^{nd}CHX$ to suppress the heat leaks. The $2^{nd}CHX$ is added to remove the excess heat from hot air. A "matching stub" is connected to the loop through a T-junction to improve the acoustic impedance matching between the engine and the refrigerator. The stub length is much less than a quarter of the wavelength.

In the thermoacoustic refrigerator, the AHX_r is also made out of an aluminium block which is 110 mm in diameter and 60 mm long. The porosity of the AHX_r is 32%. The REG_r is a stack of stainless steel mesh screens with mesh number 34 and the wire diameter 0.254 mm. The disks form a 30 mm long regenerator with a diameter of 110 mm. The porosity and hydraulic radius are 73.31% and 174.4 μm, respectively. Three Type-K thermocouples are mounted at the two ends and in the middle of the REG_r to observe the temperature distribution. The Ni-Cr resistance wire is situated at the cold side of the REG_r to act as a cooling load. The electrical power is supplied to the heater wires by a DC power supply. One Type-K thermocouple is fixed at the position of the heating wire to monitor the changes of temperature as the cooling load changes. There are six pressure transducers (PCB

PIEZOTRONICS model 122A22) placed around the loop (marked P1 to P6 in Fig. 2) to measure the pressure amplitude, phase angle and frequency. The feedback pipe (FBP) is made of standard 2-inch PVC pipe and 90° bends instead of a metal pipe to reduce cost.

In the experiments, the resonance frequency of the coupled system is 58.6 Hz. The lowest temperature of -3.6°C can be achieved at the cold end of the refrigerator with zero cooling load. In the desired temperature of +2 and +8°C for storing vital medicines , the system is capable of producing the cooling load between 3 and 7 W. Overall, the prototype would able to produce small amount of cooling capacity for storing the vital medicines [11]. Furthermore, the simulation also reported that the REG_e operates in the region of $-54.7° < \phi < -61.7°$, and the impedance phase of REG_r is in the region of $-30.5° < \phi < -16.0°$. Theoretically, the regenerator must be located within the region of travelling phasing ($-45° < \phi < +45°$) [12]. This can imply that the coupled system is non-ideal travelling wave condition to operate. This will of course affect the thermo-to-acoustic conversion or vice versa. To enhance the system performance, there are a number of issues that would need to be implemented. More specifically, these include tuning the acoustic network to improve the phase difference, selecting suitable regenerators, and investigating the optimum positions of the refrigerator and matching stub. These issues are demonstrated by modelling the coupled system in the DeltaEC programme. The acoustic field along the device is also examined. The obtained results from the present model are compared to those from the previous study [4].

4 DeltaEC simulation

In order to improve the cooling performance of the system, the optimisation process is performed using a specialized design tool namely DeltaEC [13]. Its calculation capabilities and precision in modelling thermoacoustic devices have been widely validated [14,15]. DeltaEC solves the one-dimensional wave equation based on the usual low-amplitude acoustic approximation. A solution is found for each segment, with pressures and volume flow rates matched at the junctions between segments. In the regenerators, the wave equation is solved simultaneously with the energy-flow equation in order to find the temperature profile as well as the acoustic field. The energy flowing through the regenerator is determined by temperatures and/or heat flows at adjacent heat exchangers.

In the current work, DeltaEC is used to simulate the acoustic field and the acoustic power flowing in the system. The phase angle between the acoustic pressure and velocity is tuned to achieve the travelling wave phasing. These issues are examined numerically, i.e. better matched regenerators, position and length of the stub, position of the refrigerator, etc. A block diagram of the segments in DeltaEC simulation is shown in Fig 3 (c.f. Fig. 2). The simulation for the thermoacoustic device is from the origin along the established coordinate through each segment, with pressures and volumetric velocities matched at the junctions between segments.

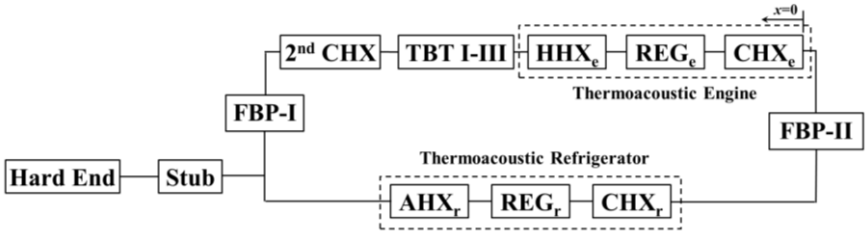

Fig. 3. The block diagram of the segments in DeltaEC simulation

The calculations are carried out under the conditions as follows: air is applied as working gas, the mean pressure is 1 bar, the hot end temperature of the engine is maintained at 700 K

and the cooling load is zero. The temperatures of all AHXs are kept at 297 K. The total length of the present model remains the same as the previous study at around 5 m. The optimisation process is subsequently executed to achieve the lowest cooling temperature of the refrigerator whilst the travelling wave phasing in both REGs is accomplished. The procedure of optimisation is performed based on the multivariable search method by varying the values of the parameters in each component.

5 Results and discussion

The simulation results discussed in this section are based on the optimised values. The comparison results between the current model and the previous study [4] are highlighted in Table 1. It can be seen that the pressure amplitude ($|p_1|$) and volumetric velocity amplitude ($|U_1|$) are improved significantly after further modification. Therefore, the acoustic power flowing in the system is also elevated. These increased outcomes are influenced by the improved acoustic impedance phases of both REGs. As can be seen from Table 1, the average phase angles in both REGs, which are -7.0° and 5.5° in the REG_e and REG_r, respectively, are close to the ideal travelling wave phase ($\phi = 0°$). This corresponds to the increase of thermo-to-acoustic efficiency of the engine, as well as the lower cooling temperature of the refrigerator.

Table 1. The simulation results

Parameters	The prototype in ref. [4]	Results from current study
Length of CHX_e	9 cm	6 cm
Position of REG_e	x = 0.104 m	x = 0.076 m
Length of REG_e	2.3 cm	3 cm
r_h of REG_e	115.2 μm	196 μm
Position of the stub	x = 1.215 m	x = 1.2486 m
Position of REG_r	x = 2.7025 m	x = 2.4105 m
Length of REG_r	3 cm	2 cm
r_h of REG_r	100 μm	120 μm
Pressure amplitude $\|p_1\|$	3.23 kPa	3.62 kPa
Velocity amplitude $\|U_1\|$	0.018 m^3/s	0.025 m^3/s
Impedance phase of REG_e	-54.7°<ϕ<-61.7°	-17.97° < ϕ <3.90°
Impedance phase of REG_r	-30.5°<ϕ<-16.0°	-1.42° < ϕ <12.47°
Efficiency of engine ($\Delta E/Q_{in}$)	5.46%	5.66%
T_{min} of the refrigerator	269 K	256 K

Fig. 4 presents the phase differences between pressure and velocity oscillating along the system. In the present study, the REG_e works in the region of -17.97° < ϕ <3.90° and the REG_r also operates in the range of -1.42° < ϕ <12.47° both of which are in the ideal travelling wave phase condition. Under the substantial adjustments, the phase differences in both REG_e and REG_r are improved significantly.

The distributions of pressure and volumetric velocity amplitudes along the system are presented in Fig. 5. It can be seen that the system performs as one-wavelength mode. The REGs are situated near the maxima of pressure amplitude or minima volumetric velocity amplitude in both models. The high acoustic impedance (ratio of acoustic pressure to velocity) is preferred in the REG to avoid high viscous dissipation. The sharp pressure drops at the REG_e and REG_r are observed due to the flow resistance of the stacked mesh screen. The present model can give a higher pressure amplitude which is up to 3.62 kPa.

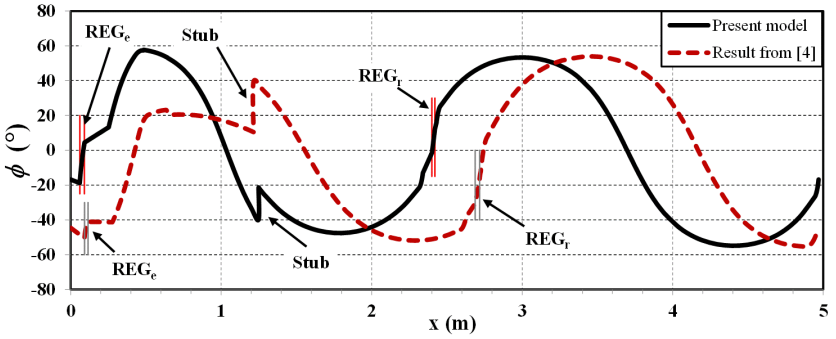

Fig 4. The distribution of phase differences between pressure and velocity along the system

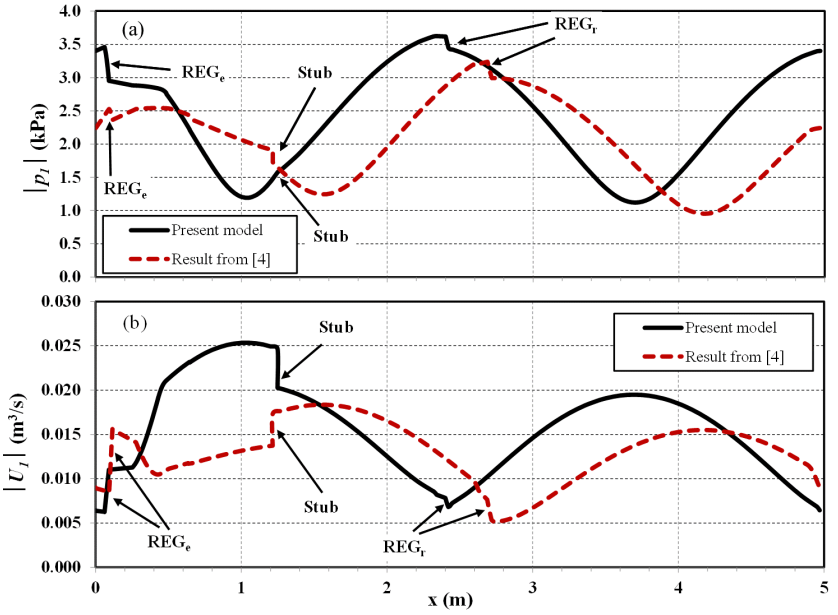

Fig. 5. The distribution of the acoustic field along the system: (a) the pressure amplitude, and (b) the volumetric velocity amplitude

Fig. 6 illustrates the acoustic power flowing along the system. In the present model, the acoustic power distributed in the system is higher. Initially at x=0, about 10.4 W of acoustic power is fed into the engine, and then amplified to around 16.4 W. Therefore, the engine can produce a net acoustic power of about 6 W at an input heat power of 106 W, corresponding to a thermo-to-acoustic conversion efficiency of 5.66%.

The HHX$_e$, TBT and 2ndCHX dissipate around 1 W of acoustic power. The acoustic power of 0.3 W is dissipated in the stub, which is much less than that of the previous model. The reason might be that the change of cross-sectional area of stub in the previous model is eliminated. Consequently, the acoustic power of 2.7 W is consumed by the refrigerator to pump heat from the cold-end to the ambient-end of the REG$_r$. The lowest temperature of 250.7 K can be achieved at no-load condition.

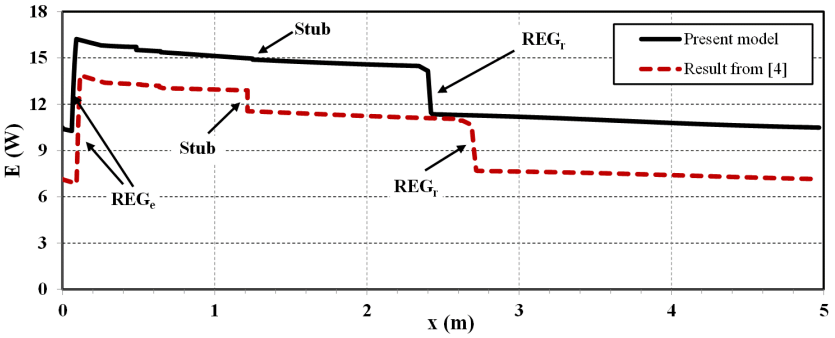

Fig. 6. The distribution of the acoustic power flowing along the system

6 Conclusions

The "coupled" configuration of the thermoacoustic engine and refrigerator in a looped-tube is studied in this work. This prototype has a high potential to be implemented for the cooling application in remote and rural area. The system is developed to be a low-cost and simple device. Formerly, the prototype was constructed and tested. The lowest cooling temperature of -3.6 ºC was produced. The experimental results indicate that this system is able to produce enough cooling power for storing small quantities of vital medicines in remote and rural areas of developing countries. However, various parameters of the prototype require further optimisation in order to obtain a higher cooling performance. Therefore, this study demonstrates further improvements of this prototype by modelling the coupled system in the DeltaEC programme. The numerical results show that after adjustment both regenerators of engine and refrigerator operate in the travelling wave phasing region with high acoustic impedance. The acoustic field in the system is also significantly improved. This contributes to a better cooling performance of the system. Further experimental investigations on the modified system are needed in order to validate the simulation results from this study.

References

1. http://www.score.uk.com/
2. G.W. Swift, J. Acoust. Soc. Am. **84**, 1145-1180 (1988)
3. A.J. Jaworski, X. Mao, Proc. IMechE, Part A: J. Power & Energy **227**, 762-782 (2013)
4. P. Saechan, H. Kang, X. Mao, A.J. Jaworski, *WCE2014*, 2097-2102 (2013)
5. K. De Blok, *Acoustic'08*, Paris, France (2008)
6. J.A. Adeff, T.J. Hofler, J. Acoust. Soc. Am. **107**, L37-L42 (2000)
7. SENER, Estrategia Nacional de Energía (2010)
8. M.A.E. Okure, *Renewable Energies in East Africa, Country Chapter: Uganda*, 1064-1133 (Deutsche Gesellschaft für Technische Zusammenarbeit (GTZ) GmbH, Eschborn, Germany, 2009)
9. Uganda Bureau of Statistics, *The National Population and Housing Census 2014 - Main Report* (2016)
10. Z. Yu, A.J. Jaworski, S. Backhaus, Appl. Energy, **99**, 135-145 (2012)
11. http://www.nrls.npsa.nhs.uk/alerts/?entryid45=66111
12. I. Dhuchakallaya, P. Saechan, P. Rattanadecho, Int. J. Energy Res. **41**, 502-511 (2017)
13. B. Ward, J. Clark, G.W. Swift, *DeltaEC programme*, LANL. (2008)
14. G.W. Swift, J. Acoust. Soc. Am. **92(3)**, 1551-1563 (1992)
15. S. Backhaus, G.W. Swift, J. Acoust. Soc. Am. **107(6)**, 3148-3166 (2000)